ISSN: 2710-0588

# Study on the Effect of Ce Doping Concentration on the Kinetics of Graphene Formation

Weifu Cen*, Xin He

School of Material Science and Engineering, Guizhou Minzu University, Guiyang, 550025, China

*Corresponding author: cenweifu1988@sina.cn

## Abstract

**The thermodynamic and kinetic processes of Ce-doped graphene were simulated by the method of first-principles molecular dynamics. The structural optimization and annealing, the kinetic properties of Ce-doped graphene composites were calculated by the classical mechanics Forcite module. The results show that with the increase of Ce doping concentration, the order of the radial distribution function in the system increases and presents a state of aggregation. According to the analysis of mean azimuth shift function, the mean square displacement (MSD) value of Ce doped graphene composite increases with the increase of doping concentration, and the corresponding diffusion coefficient also increases. The research of gyration radius and gyration evolution radius shows that with the increase of temperature and doping concentration, the gyration evolution radius of atoms becomes shorter and shorter, indicating that the interatomic force in the system is enhanced and the range of activity is shortened. Combined with the analysis of local cluster structure, it can be seen that the maximum cluster size and number of Ce doped graphene composites do not change significantly with the increase of doping concentration, indicating that Ce atom doping will improve the order in the system, increase the diffusion coefficient and enhance the interaction force between atoms. The paper aims to reduce the error between the theoretical properties and the actual properties, and provide a theoretical basis for the development of new materials with excellent properties.**

## Keywords

**Ce-doped; Graphene; Molecular Dynamics; Mean Azimuth Shift; Radial Distribution Function.**

## 1. Introduction

Materials are indispensable in people's lives, it exists and serves people in all aspects, clothing, food, housing, economic society, national development and national heavy industry construction. Under the background of the new era, new materials have also become a major chassis technology in China's manufacturing industry, even if China's new materials continue to make new breakthroughs and progress, but there are still many problems, such as China's basic materials industry still has insufficient original innovation, weak support and guarantee ability, sustainable development ability is not strong and other outstanding problems[1]. The research and development of new materials can fundamentally solve the above problems. Since the graphene material was discovered, it has been widely studied, and researchers have found that it shows better performance in all aspects, so it is also very popular with people. Graphene has high hardness strength, good stability and electrical and thermal conductivity, of which the theoretical thermal conductivity reaches 5000 W/(m•K), The theoretical Young's modulus is 1.0 TPa, the inherent tensile strength is 130 GPa, It is a new material, which is a kind of excellent

ISSN: 2710-0588

modified material, in which carbon atoms connected by $sp^2$ hybrid are tightly packed into a single two-dimensional honeycomb lattice structure [2]. It has high strength, good stability, good electrical conductivity, excellent mechanical strength and optical properties[3]. At room temperature, the carrier mobility is faster, the electron mobility is less affected by temperature changes, there is no backscattering when encountering impurities in the carrier, and the absorption rate reaches 2.3% in a wide wavelength range [4], so it is used in many fields. Such as the production of liquid crystal display screens, solar cells, biological materials, lithium batteries, semiconductor materials, early cancer diagnosis, seawater desalination filtration membranes, graphene decontamination sponges and so on[5]. In 2004 Andre K. Geim et al. [6] won the Nobel Prize in Physics after repeatedly pasting graphite with tape to obtain a single layer of graphene and designing the smallest diode. In the same year, Kostya. Novoselov and Andre.K. Geim[7] also prepared graphene. In 2008, Konstantin V. Emtsev et al[8]. also prepared optimized graphene films. In March of the same year, the Watson Research Center of International Business Machines Corporation made a low-noise graphene transistor based on SiC substrate, which shows that the application of two-layer graphene can be realized in real life; In June of the same year, Maki Suemitsu, a professor at Tohoku University in Japan, produced two graphite films with an area of $100\times150\ \mu m^2$.

In the research of graphene, a large number of scientific researchers in China have also invested in it, especially in China's relevant scientific research units and major universities and colleges, in theory, preparation, testing and other aspects have made breakthrough progress, China has made important progress in the industrialization of graphene. At present, China has established a number of graphene production enterprises, and the production capacity of these enterprises is also constantly improving. At the same time, China's graphene industry chain is also becoming more and more perfect, and research results have been widely used. Secondly, China has also made new breakthroughs in the development of graphene materials. A number of well-known scientific research institutions such as Chinese Academy of Sciences and Tsinghua University have carried out in-depth research on the development of graphene materials, and made some important achievements in the performance optimization and preparation process of graphene materials. For example, Fan Cui et al[9]. found that the anti-stray light ability of mixed spray blackening of graphene and epoxy rubber is significantly better than that of electroless nickel plating blackening. Yang Zhendong [10] synthesized a novel ionic liquid-graphene hybrid nanomaterial through the covalent interaction between ionic liquid and graphene. Zhang Huining et al. [11] found that 3D printing 3D graphene can also be well applied to water treatment. Shandong University has successfully produced a large area of graphene on a 2-inch SiC substrate.

Considering the research situation at home and abroad, it can be seen that compared with the research of graphene when it was discovered, a large number of researchers invested in the research, and its research results have made a huge leap both at home and abroad [12]. From the overall research at home and abroad, some obvious problems can be found in the major studies. It can be seen from the current development situation that its limitations are mainly reflected in the following aspects: first, there is a certain difference between the theoretical performance and the actual performance of the material, and the performance does not reach the theoretical predicted value; Second, in terms of characterization means, the degree of orientation can be directly evaluated by microscopic characterization, but there is a lack of relevant characterization means for the influence of microscopic structure on macro performance. Therefore, in this paper, the selection of Ce doping to regulate the physical and chemical properties of graphene and the kinetic mechanism of doping formation process are studied.

ISSN: 2710-0588

# 2. Calculation Method and Model

## 2.1. Calculation Model

Where, Ce is a square crystal, the density is 6.9 g/cm$^3$ [13]. The structure of Ce doped into graphene is a cubic crystal system, and the symmetric elements are four cubic rotation axes [14], all of which are symmetric $P_1$[15]. The specific cell constants are shown in Table 1 and Table 2.

**Table 1.** Cell parameters at different doping concentrations at 300 K

| Concentration | a/Å | b/Å | c/Å | α/° | β/° | γ/° |
|---|---|---|---|---|---|---|
| 1% | 40.58 | 40.58 | 40.58 | 90.00 | 90.00 | 90.00 |
| 2% | 41.94 | 41.94 | 41.94 | 90.00 | 90.00 | 90.00 |
| 3% | 43.23 | 43.23 | 43.23 | 90.00 | 90.00 | 90.00 |

**Table 2.** the Mass, volume and number of particles at different doping concentrations at 300 K

| Concentration | Density /(g/cm3) | Volume / Å | Population of particles |
|---|---|---|---|
| 1% | 1.00000 | 66814.4 | 3030 |
| 2% | 1.00000 | 73794.7 | 3060 |
| 3% | 1.00000 | 80774.9 | 3090 |

Figure 1 is the structural model diagram of Ce doped graphene, the gray sphere represents graphene, and the yellow sphere represents Ce. Due to the difference in Ce doping amount, the proportion of different colors can be clearly seen. (a) the doping concentration is 1% and the structural model is 300K; (b) the doping concentration is 2% and the structural model is 300K. (c) is a structural model with a doping concentration of 3% and 300 K.

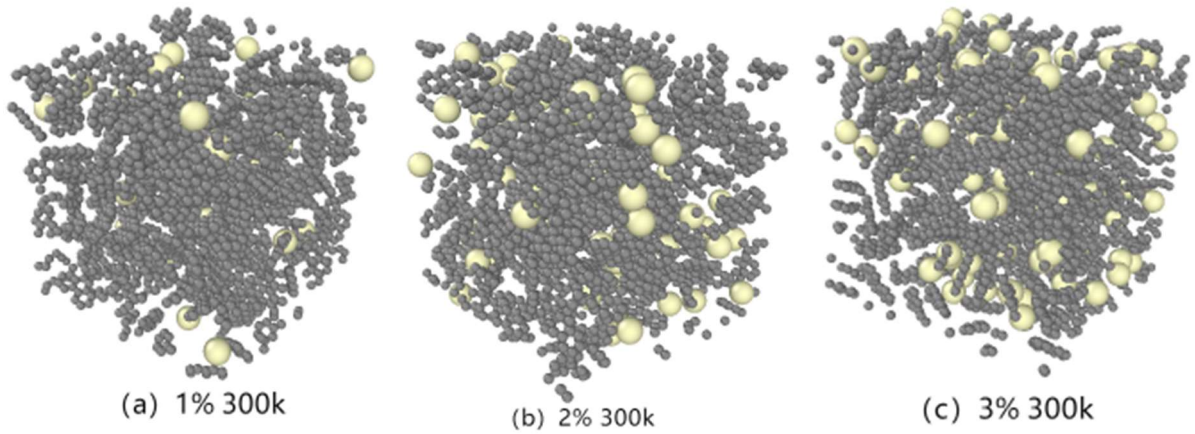


**Figure 1.** The structural model of Ce doped graphene (a) is the structural model at a doping concentration of 1% and 300K, (b) is the structural model at a doping concentration of 2% and 300K, and (c) is the structural model at a doping concentration of 3% and 300K

## 2.2. Calculation Parameters

Three groups of graphene with different doping concentrations were annealed at an initial temperature of 300 K [16]. The annealing cycles were 5 times, the mid-cycle temperature (the highest part of the cyclic annealing) was 2000 K, and the temperature gradient steps of the cooling process in one cycle were 20, and the kinetic steps of each temperature gradient were

ISSN: 2710-0588

100. The total number of kinetic steps is 2000, and the optimized structure is annealed. In the kinetic parameters, the micro regular NVE ensemble is adopted (the number of atoms, volume and energy of the system are constant) [17-20], the step size is 1.00 fs, and the initial velocity is randomly default. In the energy parameters, the Universal force field of the system is selected, and the simulation method of Ewald's ball method is adopted [21]. The accuracy is kept at 0.001 kcal/mol, and the buffer width distance is 0.5 Å [22].

## 3. Results and Discussion

### 3.1. Dynamic Characteristic Analysis

In order to obtain more accurate data, Anneal module is used in this paper to anneal the initial model above. Anneal is annealed at an initial temperature of 300 K, the number of annealing cycles is 5 times, the temperature in the middle of the cycle (the hottest part of the cycle annealing) is 2000 K, and the number of temperature gradient steps in the process of heat reduction in one cycle is 20. The number of dynamic steps for each temperature gradient is 100, and the total number of dynamic steps is 2000, and the optimized structure is annealed. Figure 2 simulated running annealing process.

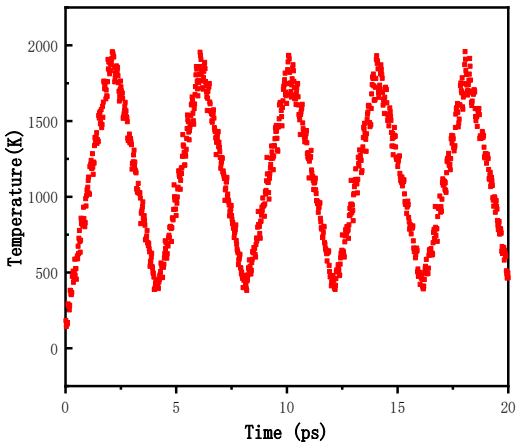


**Figure 2.** Function relationship between temperature and time during simulated annealing

After annealing is completed, Dynamics module is used for dynamic analysis of the model, and whether the system tends to be stable is analyzed through the output energy and temperature change trend diagram. In the NPT ensemble simulated by molecular dynamics, the balance of the system is judged through energy fluctuations. If the change amplitude of the total potential energy is within 10%, the system can be judged to have reached equilibrium [2], indicating that the temperature and energy of the system have reached a stable state, then the analysis can be carried out.

### 3.2. Radial Distribution Function

In the radial distribution function (RDF), when the order of an RDF structure is strong, it will form a distinct peak. The height and sharpness of this peak can reflect the degree of order of the RDF structure. If the peak is high and sharp, it indicates that the connection between the atoms is relatively close and the structure is more orderly. On the contrary, if the peak is short and flat, it indicates that the structure are more loose and disordered. In other words, by analyzing RDF values and their distribution, the structure and tight aggregation characteristics

ISSN: 2710-0588

in the whole system can be predicted [23]. As r increases indefinitely, the value of g(r) tends to 1[24]. The mathematical formula for RDF is as follows:

$$g(r) = \frac{\rho(r)}{\rho} \tag{1}$$

Where, $\rho(r)$ is the particle density in the crystal.

In the RDF graph, the closer the position of the first peak value is to the Y-axis and the higher the smoothness indicates that the binding ability is stronger there, and the system may show a state of aggregation. If it is far away from the y axis or not obvious, it indicates that the binding force is weak and the system may present a discrete state. For a tightly packed system, g(r) will quickly peak and then decrease to 1. The integral of g(r) at the first peak is the average number of particles in the shell there. Figure 3 is the RDF diagram of graphene at different doping concentrations. From the diagram, we can see that when the central atomic distance is 1.41 Å, its radial distribution function has a maximum value of 32.34. The results show that when r=1.41 Å, the interaction force between the central atom and the adjacent atom is the strongest, which shows the short-range order and aggregation state, and also indicates that the average particle number reaches the maximum. The number of separated peaks represents the position of particles on the lattice point, that is, there are 5. With the increase of radius, the radial distribution function gradually tends to 1, indicating that the interaction force between atoms is very weak, and the system has reached stability.

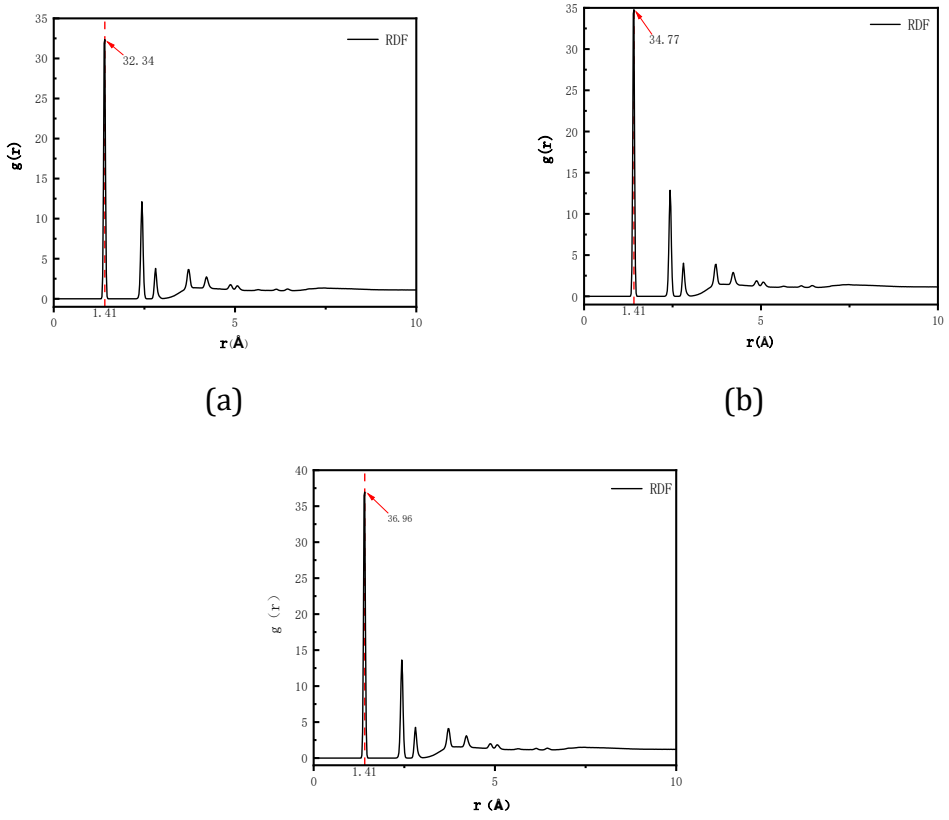


(a) (b)

(c)

**Figure 3.** RDF at different doping concentrations of 300 K, (a)1%, (b)2%, (c)3%

ISSN: 2710-0588

## 3.3. Mean Square Displacement

MSD is the mean azimuth shift, that is, in the process of molecular dynamics simulation, the particles do irregular thermal motion from the initial time, and the average displacement of the particles in a certain period of time is the mean azimuth shift [24]. It corresponds to the diffusion coefficient of atoms. In practice, the statistical data will decrease with the time interval, usually producing a large fluctuation at the end. Through the mean azimuth shift analysis, the change of the diffusion coefficient with temperature is obtained. The increase of MSD over time is related to the diffusion coefficient D, expressed as follows:

$$r^2(t) = \frac{1}{N}\left(\sum_{k=0}^{n}\sum_{i=1}^{N}|r_i(t) - r_i(0)|\right) \tag{2}$$

According to Einstein's diffusion law, the following expression can be obtained:

$$\lim_{t\to\infty}(r)^2 = C + 6Dt \tag{3}$$

Where r is the mean azimuth shift function, D is the diffusion coefficient, and C is the constant.

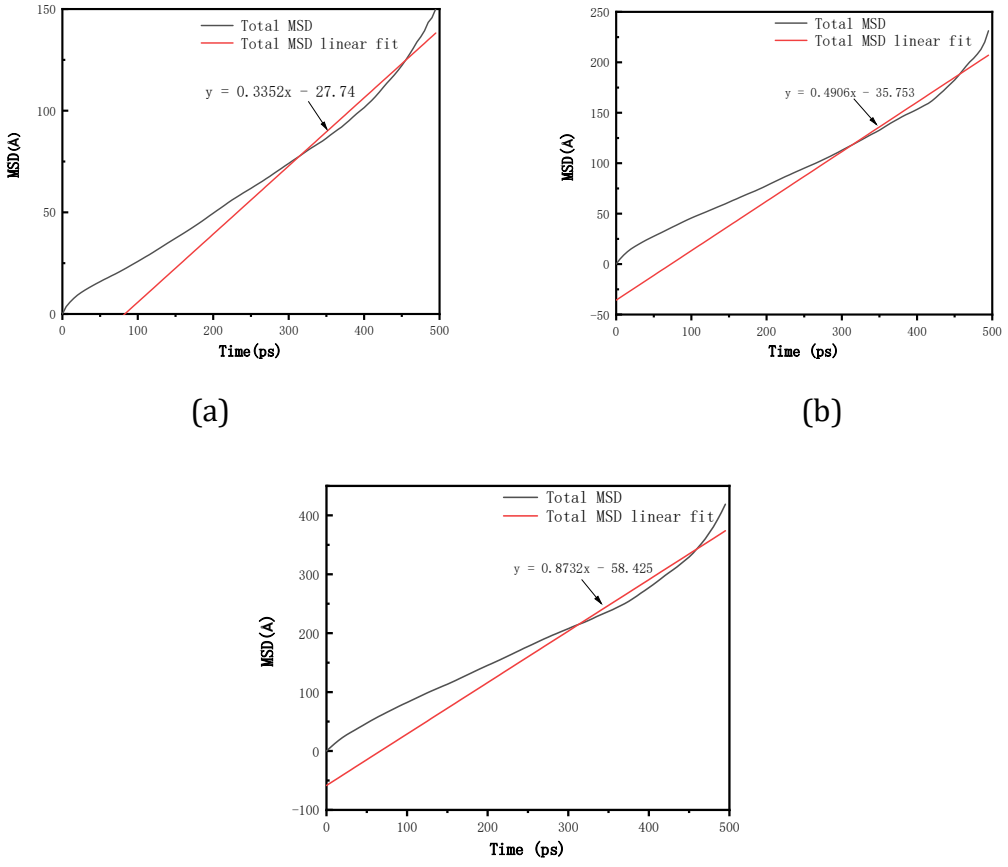


(a) (b)

(c)

**Figure 4.** MSD at different doping concentrations of 300 K, (a)1%, (b)2%, (c)3%

Figure 4 is the MSD diagram at different doping concentrations of 300 K, and Figure 4(a) is the MSD diagram at 1% 300 K, where the black is the MSD curve and the red is the fitted MSD curve. The origin curve fitting tool can tell that the fitted curve expression is y = 0.3352x-27.74.

ISSN: 2710-0588

Through calculation, the diffusion coefficient can be obtained from the mean azimuth shift curve as 0.05586930 Å $^2$/ps, which is converted to 0.97130160 cm$^2$/s. Figure 4(b) 2% 300K MSD diagram, in which the black is the MSD curve and the red is the fitted MSD curve. The origin curve fitting tool shows that the fitted curve expression is y = 0.4906x-35.753. After calculation, the diffusion coefficient can be obtained from the mean azimuth shift curve as 0.08176070 Å $^2$/ps, which is converted to 0.96774486 cm$^2$/s. Figure 4(c) is the MSD diagram at 3% 300K, in which the black one is the MSD curve and the red one is the fitted MSD curve. It can be seen from the origin curve fitting tool that the fitted curve expression is y = 0.8732x-58.425. The diffusion coefficient can be obtained from the mean azimuth shift curve as 0.14553724 Å $^2$/ps, which is converted to 0.95417058 cm$^2$/s. In conclusion, with the addition of Ce atom, the diffusion coefficient in the system increases and the diffusion capacity becomes stronger, which is mainly shown as $1.455\times10^{-7}>0.818\times10^{-7}>0.559\times10^{-7}$.

## 3.4. Radius of Rotation and Radius of Rotation Evolution

The radius of rotation generally also refers to the radius of inertia, which refers to the distance between the axis of rotation concentrated around the center of the object, its value is the square root value of the moment of inertia of any section to a certain axis divided by the area of the section [24], the expression is:

$$r = \frac{\sqrt{D^2 - d^2}}{4} \tag{4}$$

In this study, we studied and discussed the interaction of atoms in the system under different doping concentrations by output probability density function images and gyroradius function images, so as to analyze the overall properties of atoms in the system.

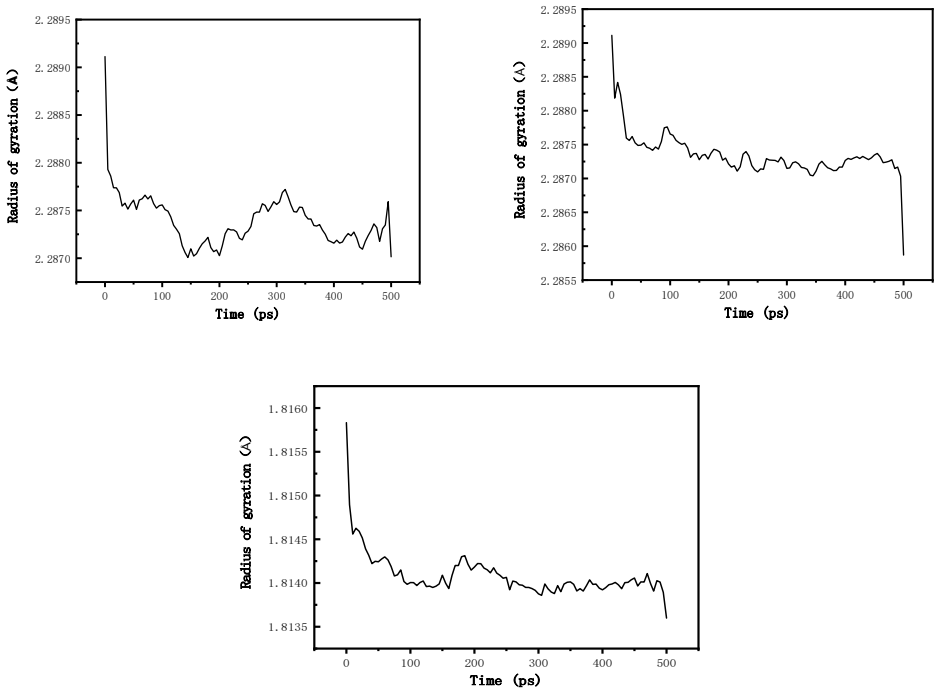


**Figure 5.** Cyclotron evolution radius at different doping concentrations of 300 K, (a)1%, (b)2%, (c)3%

ISSN: 2710-0588

Figure. 5(a) 1% 300 K cyclotron evolution radius diagram, from which it can be seen that in the running 500 ps, the gyroscope of the system shows A general downward trend, the highest gyroscope is 2.2891 Å, the lowest is 2.2868 Å, and the range of the gyroscope remains between 2.2868 and 2.2891. The range of cyclotron radius of the output probability density function graph is mostly kept in 2.46~2.79. Both the single probability density image and the gyration evolution radius image show that the gyration radius of the atoms in the system keeps within a certain value range and has a downward trend, indicating that the binding force of the atoms in the system is getting stronger and stronger. Figure. 5(b) is the cyclotron evolution radius diagram at 2% 300 K. It can be seen from the diagram that during the operation of 500 ps, the rotation radius in the system generally presents A downward trend, with the highest rotation radius being 2.2891 Å and the lowest being 2.2858 Å. Moreover, the range of cyclotron radius is kept between 2.2858 and 2.2891, and the range of cyclotron radius of the output probability density function graph is mostly kept between 2.47 and 2.79. Both the single probability density image and the gyrotron evolution radius image show that the cyclotron radius of atoms in the system is kept within a certain value range and has a downward trend. It shows that the binding force of atoms in the system is getting stronger and stronger. Figure. 5(c) is 3% 300K cyclotron evolution radius diagram. It can be seen from the diagram that in the 500 ps operation, the gyroscope of the system generally presents A downward trend, with the highest gyroscope being 1.8158 Å and the lowest being 1.8136 Å, and the range of gyroscope is maintained between 1.8136 and 1.8158. The range of cyclotron radius of the output probability density function graph is mostly kept in 2.47~2.79. Both the single probability density image and the gyrotron evolution radius image show that the cyclotron radius of the atoms in the system is kept in a certain numerical range and has a downward trend, indicating that the binding force of the atoms in the system is getting stronger and stronger. In summary, with the increase of Ce concentration, the gyroradius becomes smaller and smaller, showing 2.2868 Å > 2.2858 Å > 1.8136 Å. Therefore, it is concluded that the addition of Ce atoms makes the binding force in the system more and more strong, showing aggregation.

## 3.5. Local Cluster Structure Analysis

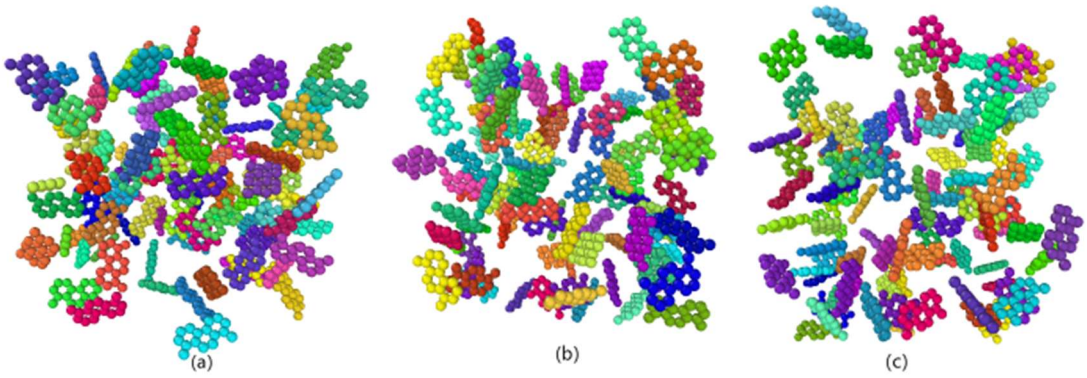


**Figure 6.** 300 K is the local cluster structure of Ce-doped graphene (a)1%, (b)2%, (c)3%

Under the condition of 1% 300 k, the system has 3030 atoms and 230 types of clusters, including 16, 14 and 1 size types, among which 100 clusters with 16 size are proposed. Therefore, the large and large size clusters of the system are obtained, as shown in Figure 6 (a), which consists of 100 clusters and 1600 atoms. Under the condition of 2% 300 k, the system has 3060 atoms and 260 types of clusters, including 16, 14 and 1 size types, among which 100 clusters with 16 size are proposed. For this reason, the large and large size clusters of the system are obtained, as shown in Figure 6 (b), which consists of 100 clusters and 1600 atoms. Under the condition of 3% 300 k, the system has 3090 atoms and 290 types of clusters, including 16, 14 and 1 size types, among which 100 clusters with 16 size are proposed.

ISSN: 2710-0588

Therefore, the large and large size clusters of the system are obtained, as shown in Figure 6 (c) above, which consists of 100 clusters and 1600 atoms. In summary, combined with the output file, it is inferred that Ce doping does not cause changes in cluster size, and the doped Ce atom forms a single cluster, which is why the cluster type increases with the increase of doping concentration.

## 4. Conclusion

In this paper, the classical dynamics module Forcite in Material Studio was used to conduct dynamic research on the simulated kinetic model of Ce doped graphene composite. After annealing, the kinetic calculation was carried out, and the force distribution of atoms inside the composite was simulated through the radial distribution function. The diffusion coefficient of the composite was simulated by the mean azimuth shift. The internal aggregation and dispersion of atoms are simulated by the gyration radius and gyration evolution radius, and then the Cluster analysis in ovito software is used to analyze the internal cluster of atoms. After the Ce doping concentration of 1%, 2% and 3% of the systems were respectively studied, their radial distribution function, mean azimuth shift, rotation radius and rotation evolution radius were obtained: (1) With the incorporation of Ce atoms, the structure order in the system is improved. (2) With the incorporation of Ce atoms, the bond in the system is closer and appears as an aggregation state. (3) With the incorporation of Ce atoms, the diffusion coefficient increases and the diffusion capacity becomes stronger. (4) The doping of Ce atoms does not affect the existing clusters in the system, indicating that the incorporation of Ce atoms will make the force of each cluster stronger, making the architecture more compact.

## Acknowledgments

This work was supported by the PhD initial foundation of Guizhou MinZu University (GZMUZK[2024]QD17), the Youth Science and Technology Talents Growth Fund Program of the Ministry of Education Province, China (NO.[2022]155).

## Data Availability Statement

The data that support the findings of this study are available on request from the corresponding author.

## References

[1] Du Zhi-xiong, Li Jia-jia, Guo Yan. Speed up the construction of agricultural power should focus on the direction of breakthrough [J].Theoretical discussion, 2023, No.232(03): 154-162.

[2] Zheng K. Molecular dynamics simulation of thermal properties of graphene [D]. Dalian University of Technology, 2015.

[3] Zhang Zhifang. Preparation and electrochemical properties of graphene/transition metal compound composites [D]. Shanghai University of Electric Power, 2020.

[4] Chen Jinlong. Preparation of graphene and its application in chemical/biological sensing [D]. Nankai University, 2011.

[5] Wu H. Synthesis and properties of surface ionic imprinting of rare earth element ion cerium [D]. Jiangxi Normal University, 2014.

[6] Novoselov K S, Geim A K, Morozov s v, et al. Electricfield effect in atomically thin carbon films[J]. Science,2004, 306(5296):666.

[7] Anonymous. Vanderbilt University; Tuning graphene film so it sheds water[J]. NewsRx Health & Science, 2011.

ISSN: 2710-0588

[8] Matthias Scheffler,Wolf-Dieter Schneider. Focus on Advances in Surface and Interface Science[J]. New Journal of Physics, 2007, 9(10).

[9] Fan Cui, Mo Defeng, Wang Xiaokun, et al. Comparison of properties of graphene spray and electroless nickel blackening cold screen [J]. surface technology, 2022, (009):051.

[10] Yang Zhendong. Passivation behavior of bogie steel and study on its protective properties of graphene epoxy coating [D]. Ningbo Institute of Materials Technology and Engineering, University of Chinese Academy of Sciences), 2020.

[11] Zhang H N, Shi Z Y, Xiao Y K. 3D printing preparation of three-dimensional graphene and its application in water treatment [J]. Progress in chemical industry, 2022, 41(05):2231-2242.

[12] ALLEN M P, TILDESLEY D J. Computer simulation of liquids [M]. Oxford: Oxford University Press, 1989.

[13] Zhao Su, Li Jinfu, Zhou Yaohe. Molecular dynamics simulation and its application in materials science [J]. Material guide, 2007(4) : 5-8+25.

[14] Tan Min. Molecular dynamics simulation of directionally induced growth of GaN twin structures [D]. Guizhou University, 2022.

[15] Nosé S. A unified formulation of the constant temperature molecular dynamics methods[J]. The Journal of chemical physics, 1984, 81(1):511-519.

[16] Woodcock L V. Isothermal molecular dynamics calculations for liquid salts[J]. Chemical Physics Letters, 1971, 10(3): 257-261.

[17] Evans D J, Hoover W G, Failor B H, et al. Nonequilibrium molecular dynamics via Gauss's principle of least constraint[J]. Physical Review A, 1983, 28(2):1016.

[18] Tian Ze 'an. Simulation of solidification process and microstructure evolution of liquid silver metal [D]. Hunan University, 2009.

[19] Sun H . Force field for computation of conformational energies, structures, and vibrational frequencies of aromatic polyesters[J]. Journal of Computational Chemistry, 1994.

[20] Wang Haipeng, Wang Qing. Teaching method for characterizing two-body distribution functions of liquid metal structures [J]. Physics and engineering, 2022, 32(01): 155-161.

[21] Zhang Yan-ning, Wang Li, Bian Xiu-fang. Molecular dynamics simulation of intermediate-scale Au nanocluster solidification process [J]. journal of synthetic crystals,2003, (01):50-54.

[22] Zhou G H, Zhao T H, Wan J, et al. Predict the glass transition temperature and plasticization ofβ-cyclodextrin/water binary system by molecular dynamics simulation[J]. Carbohydrate Research, 2015, 401:89-95.

[23] Liu Jin. Molecular dynamics simulation of crystallization and mechanical properties of graphene and polyethylene composites [D]. Taiyuan University of Technology, 2020.

[24] Zhang Yonghao. Molecular dynamics simulation of microstructure of MgO-Al2O3-SiO2-TiO 2 glass-ceramics [D]. Shandong University of Architecture and Engineering, 2019.